

Cell separation by the combination of microfluidics and optical trapping force on a microchip

Masaya Murata · Yukihiro Okamoto · Yeon-Su Park ·
Noritada Kaji · Manabu Tokeshi · Yoshinobu Baba

Received: 28 October 2008 / Revised: 22 December 2008 / Accepted: 23 January 2009 / Published online: 19 February 2009
© Springer-Verlag 2009

Abstract We investigated properties of cells affecting their optical trapping force and successfully established a novel cell separation method based on the combined use of optical trapping force and microfluidics on a microchip. Our investigations reveal that the morphology, size, light absorption, and refractive index of cells are important factors affecting their optical trapping force. A sheath flow of sample solutions created in a microchip made sample cells flow in a narrow linear stream and an optical trap created by a highly focused laser beam captured only target cells and altered their trajectory, resulting in high-efficiency cell separation. An optimum balance between optical trapping force and sample flow rate was essential to achieve high cell separation efficiency. Our investigations clearly indicate that the on-chip



Yukihiro Okamoto has been an Assistant Professor at Nagoya University since April 2008. His current research interests are the development of functional materials and their application to high-performance biomolecule analysis.

M. Murata · Y. Okamoto (✉) · N. Kaji · M. Tokeshi · Y. Baba
Department of Applied Chemistry,
Graduate School of Engineering, Nagoya University,
Nagoya 464–8603, Japan
e-mail: yokamoto@apchem.nagoya-u.ac.jp

Y. Okamoto · Y.-S. Park · N. Kaji · M. Tokeshi · Y. Baba
MEXT Innovative Research Center for Preventive Medical
Engineering, Nagoya University,
Nagoya 464–8603, Japan

Y. Baba
Plasma Nanotechnology Research Center, Nagoya University,
Nagoya 464–8603, Japan

Y. Baba
Health Technology Research Center, National Institute of
Advanced Industrial Science and Technology (AIST),
Takamatsu 761–0395, Japan

Y. Baba
Institute for Molecular Science,
National Institutes of Natural Sciences,
Okazaki 444–8585, Japan

optical trapping method allows high-efficiency cell separation without cumbersome and time-consuming cell pretreatments. In addition, our on-chip optical trapping method requires small amounts of sample and may permit high-throughput cell separation and integration of other functions on microchips.

Keywords Optical trapping · Microchip · Cell separation · Sheath flow · Trapping force

Abbreviations

| | |
|--------|----------------------------------|
| DNA | deoxyribonucleic acid |
| FBS | fetal bovine serum |
| DMEM | Dulbecco's modified Eagle medium |
| UV-Vis | ultraviolet and visible |
| FOM | figure of merit |

Introduction

Separation of specific target cells is important in clinical diagnoses and regenerative medicine [1]. In this regard,

various cell separation methods have been investigated, including density gradient centrifugation [2], electrophoresis [3], magnetic separation [4], and fluorescent activated cell sorter (FACS) [5]. Unfortunately, these methods lack one or more of the following important requirements: simplicity, high-throughput capability, high accuracy, cost-effectiveness, and noninvasiveness, which allow for simple, convenient, economical, and high-throughput cell separation. Recently, extensive research on cell separation methods has focused on the combination of microchips [6] with one of the conventional cell separation techniques, such as magnetic separation [7], FACS [8], dielectrophoresis [9], aqueous two-phase distribution [10], chromatography [11], and size separation with pillars [12], because the on-chip methods require very small amounts of sample and enable high-throughput analyses. Despite its many advantages, cell separation with microchips still needs time-consuming and cumbersome sample pretreatments such as purification, concentration, or reaction with dyes or magnetic beads. Therefore, simple and easy methods for high-performance cell separation are in great demand.

Optical trapping or optical tweezers [13, 14] can manipulate nanometer- and micrometer-sized dielectric particles. Optical trapping uses a tightly focused beam of light to stably hold microscopic particles in three dimensions with approximately piconewton force. It is a contactless and noninvasive technique and provides the possibility for separating and concentrating target cells from the others without labor-intensive and time-consuming cell pretreatments. In these regards, optical trapping is considered as one of the promising candidates for novel cell manipulation and separation, and the technique has been successfully applied to manipulate biological samples such as viruses, bacteria [15], cells [16], and DNA [17, 18]. Optical trapping requires each cell to be approached within the boundary of a focused laser beam, which hinders application of the technique to high-throughput cell separation and concentration; however, combined use of optical trapping and a microchip can provide a nice solution to this problem. In a microchannel of the microchip, a sheath flow can be easily created to line up cells in a row, and then optical trapping can be used to separate and concentrate cells depending on their optical trapping ability.

Here, we demonstrate the usefulness of our novel approach, the combination of optical trapping and microchips, for high-throughput cell separation and concentration. Initially, our investigations were focused on basic aspects of optical trapping-based cell separation, especially on various factors affecting optical trapping of cells. After that, our focus moved to the generation of a sheath flow of sample solutions in a microchannel to permit sample cells to flow in a line and enter into the focused laser spot, resulting in successful separation of cells. Finally, we investigated the

effect of various parameters such as laser power and sample flow rate on cell separation efficiency.

Experimental

Materials

Polystyrene beads (2.65%, diameter 6.0, 10.0, 15.0, and 25.0 μm), and glass beads (refractive index 1.51, diameter 3.0–10.0 μm) were purchased from Polysciences (Warrington, PA, USA). These particles were diluted 100-fold with deionized water before use. Glass beads with 6.0- μm diameter were selected based on their image size on a video monitor (Sony, Tokyo, Japan) and used for trapping force measurements. Trypan blue and erythrosin B were from Sigma (St. Louis, MO, USA) and Merck (Darmstadt, Germany), respectively. Poly(methyl methacrylate) (PMMA) microchips were obtained from Hitachi Chemicals (Tokyo, Japan); PMMA microchips have excellent optical properties compared with other polymer microchips; their detailed schematic layout is shown in Fig. 1 and described in our previous report [19].

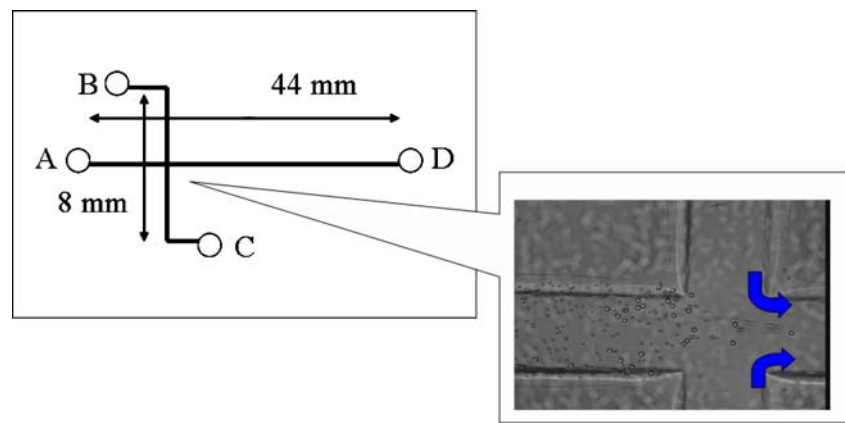
Cell culture and sample cell preparation

HeLa cells were cultured in Dulbecco's modified Eagle medium (DMEM) (Invitrogen, Carlsbad, CA) supplemented with 10% fetal bovine serum (FBS) (Invitrogen), 1% antibiotic-antimycotic solution (Nacalai tesque, Kyoto, Japan), and 1% 200 mM L-glutamine (MP Biomedical, Inc, Costa Mesa, CA, USA) at 37 °C under 5% CO₂. NCB and HL-60 cells were cultured in RPMI 1640 (Invitrogen) supplemented with 10% FBS and in Iscove's modified Dulbecco's medium (Sigma) with 20% FBS at 37 °C under 5% CO₂, respectively. Before the experiment, HeLa cells were harvested from culture dishes with trypsin-ethylenediaminetetraacetic acid solution (Invitrogen), washed by centrifugation, and redispersed in DMEM. Dead HeLa cells were prepared as follows: 1 mL of 2.5×10^6 live cells was mixed with 40 μL of 0.4% trypan blue solution or 40 μL of 0.5% erythrosin B solution and then stored at 4 °C overnight.

Optical trapping

The optical trapping method employed is almost the same as in our previous reports [17]. Briefly, optical trapping was performed with PALM[®] Robot-Micro Tweezers (P.A.L.M. AG Microlaser technologies, Bernried, Germany), which is composed of a microscope, video camera, and laser. Images of the trapped and separated cells were obtained with the Axiovert S100TV fluorescent microscope (Carl Zeiss Jena

Fig. 1 Schematic of a poly (methyl methacrylate) microchip. *A–C* sample injection reservoirs, *D* waste reservoir, *thick black lines* microchannels. The *inset* shows a sheath flow near the cross intersection of the microchannels (*blue arrows* flow direction)



GmbH, Jena, Germany) equipped with a $\times 40$ objective lens (numerical aperture 0.75). A continuous wave mode of a neodymium vanadate laser (1,064 nm, Coherent, Inc. Laser Group, Santa Clara, CA, USA) was employed for laser trapping.

UV–Vis absorption spectra of samples were obtained with a UV-3600 spectrophotometer (Shimadzu, Kyoto, Japan).

Separation of dead and live HeLa cells

To prepare sample suspensions of mixed cells, one part of the trypan blue-stained dead cells was mixed with one part of the unstained live cells. In each experiment, 10 μL of the cell suspension was injected into the reservoir A while 30 μL of water was injected into the reservoirs B and C, as shown in Fig. 1. This procedure generated a sheath flow from the cross intersection of the corresponding microchannels and focused all the sample cells into a narrow stream. Only live cells were optically trapped by the focused laser beam, which changed their trajectories into the downstream from the cross intersection, and finally separated them from dead cells. Separation efficiency was estimated by counting the number of live cells (and also dead cells) altering or maintaining their trajectories on the captured motion picture.

Estimation of optical trapping force

Optical trapping force was measured according to our previous report [17]. Briefly, 10 μL of sample solution was injected into each of the inlet reservoirs (A–C); upon injection, the sample solution started to move toward the outlet as a result of capillary force; movement of the samples in the solution stopped in the microchannel a few minutes later due to the establishment of dynamic equilibrium. After achieving this equilibrium condition, a focused laser beam (1,064-nm wavelength, 1- or 3-W power) was irradiated on the target sample, and optically trapped sample was then immediately dragged by a microscope

stage moving linearly for a distance of 200 μm (round trip) at arbitrary constant velocity. As the drag velocity increased, the trapped sample was removed from the optical trap by hydrodynamic force at a specific velocity. This velocity was recorded to estimate the optical trapping force. Optical trapping force was estimated by using Stokes' law based on the drag force induced by moving the surrounding medium:

$$F_t = F_D = 6\pi\eta r v_c$$

where F_t is the trapping force, F_D the drag force on the sphere, η the viscosity of the surrounding medium, r the radius of the sphere, and v_c the critical velocity defined as the velocity at which the sphere is removed from the optical trap as a result of a given drag force.

Results and discussion

In principle, many factors can influence the trapping forces, but major factors are cell morphology, size [20], degree of laser absorption [21–23], and refractive index [24]. The aforementioned papers reported the effect of only one physical property on the optical trapping force and did not investigate the effect of a series of important factors systematically. To understand how strongly each physical property of the cells contributes to their optical trapping, we have done comprehensive investigations on the effect of a series of physical properties of the cells.

Estimated optical trapping forces of the cells tested are summarized in Table 1. The trapping forces of the unstained live cells were different from each other: 7.9, 11.3, and 22.5 pN for HeLa, HL-60, and NCB cells, respectively. These differences can be mainly attributed to the size and morphology of the cells [20]. To confirm the size effect on optical trapping forces, we estimated the optical trapping forces of spherical polystyrene beads with different diameters (6, 10, 15, and 25 μm) as model samples. The optical trapping force increases as the size of the beads increases, as shown in Table 2. Thus, it is clear

Table 1 Optical trapping force of various cells

| Cells | HeLa cells | | | NCB cells | HL-60 cells |
|--|------------|---------------------|----------------------|-----------|-------------|
| | Unstained | Trypan blue stained | Erythrosin B stained | Unstained | Unstained |
| Optical trapping force (pN) ^a | 7.9 | 5.3 | 6.2 | 22.5 | 11.3 |

Laser power 3.0 W

^a Average value for ten samples

that the size of samples has a strong effect on the trapping force. However, the size of HeLa cells (ca. 7.5 μm) is bigger than those of HL-60 (ca. 5.0 μm) and NCB cells (ca. 6.0 μm), whereas the trapping force of HeLa cells is smaller than those of HL-60 and NCB cells. This can be explained by the differences in their cell morphology: HeLa cells are nonspherical, whereas NCB and HL-60 cells are almost spherical. These differences in the trapping force, caused by the differences in the size and morphology of the cells, might be useful for separating cells having different sizes and/or morphology without special cell pretreatments, such as staining and purification, and might permit high-throughput cell separation.

Degree of light absorption and refractive index can also affect optical trapping ability of the samples. To investigate these possibilities, we stained HeLa cells with dyes having different absorption features (trypan blue and erythrosin B) and then performed optical trapping experiments. Table 1 summarizes the results. Staining HeLa cells with trypan blue or erythrosin B caused a decrease in the trapping force, as compared with corresponding unstained live cells. This decrease might be attributed to the light absorption and/or refractive index change. When laser light is absorbed by dielectric particles or medium, heat generation occurs [21–23]. This decreases viscosity of the surrounding medium and enhances Brownian motion and convection of the medium, resulting in a decrease in the trapping force. The light absorption also changes the momentum of photons, resulting in reduced optical trapping force. In addition to the light absorption, refractive index also affects the trapping force. To investigate these possibilities in detail, a series of optical trapping force measurements and spectrophotometric analyses were performed.

Table 2 Optical trapping force of various microspheres

| Microsphere | Polystyrene beads | | | | Glass beads |
|----------------------------------|-------------------|------|------|------|-------------|
| | 6.0 | 10.0 | 15.0 | 25.0 | 6.0 |
| Trapping force (pN) ^a | 5.1 | 5.7 | 8.3 | 21.1 | 4.0 |

Laser power 1.0 W

^a Average value for ten samples

When a focused beam of a high power laser is employed, two-photon absorption could occur [25]. Therefore, we must consider two different absorption processes: simple absorption at 1,064 nm and two-photon absorption at 532 nm. Absorption at 1,064 nm can be ruled out from the consideration because neither of the sample cells has an absorption at this wavelength, as shown in the ultraviolet (UV)–near-infrared (NIR) spectra in Fig. 2; thus, only two-photon absorption can be considered. As can be seen in Table 1, the optical trapping forces of the stained dead HeLa cells are smaller than that of unstained live HeLa cells. This can be partially attributed to the fact that the stained dead cells have much higher light absorption at 532 nm than unstained live cells. The overall order of optical trapping force, measured at the same concentration of the samples, is as follows: unstained live cells > erythrosin B-stained dead cells > trypan blue-stained dead cells. Interestingly, the trypan blue-stained dead HeLa cells show weaker optical trapping force than the erythrosin B-stained dead HeLa cells, in spite of weaker light absorption by the former than by the latter. This fact signifies that refractive index of the samples, in addition to the degree of light absorption, is an important factor for determining their optical trapping forces as described below.

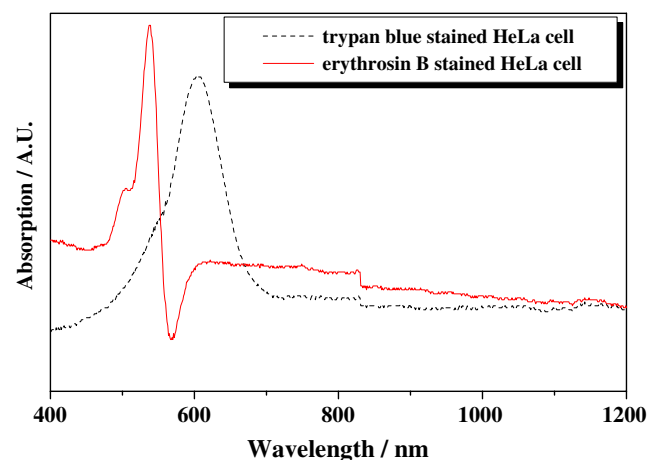
**Fig. 2** UV–NIR spectra of dead HeLa cells stained with trypan blue and erythrosin B

Fig. 3 Effect of flow rate and laser power on the separation of dead and live HeLa cells

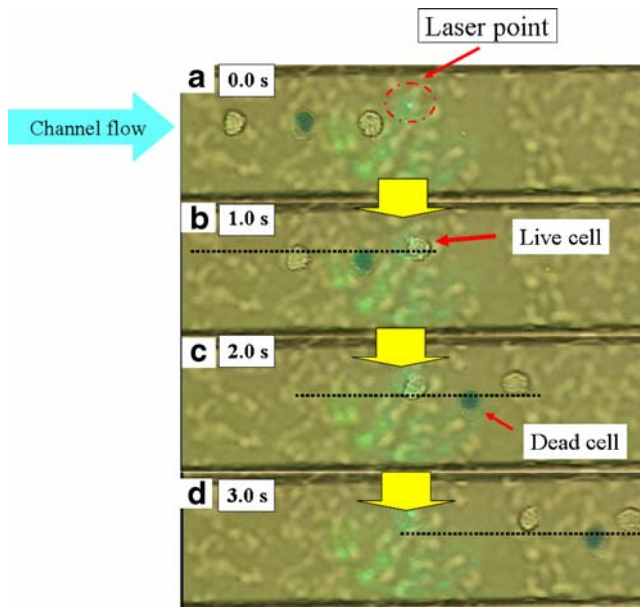
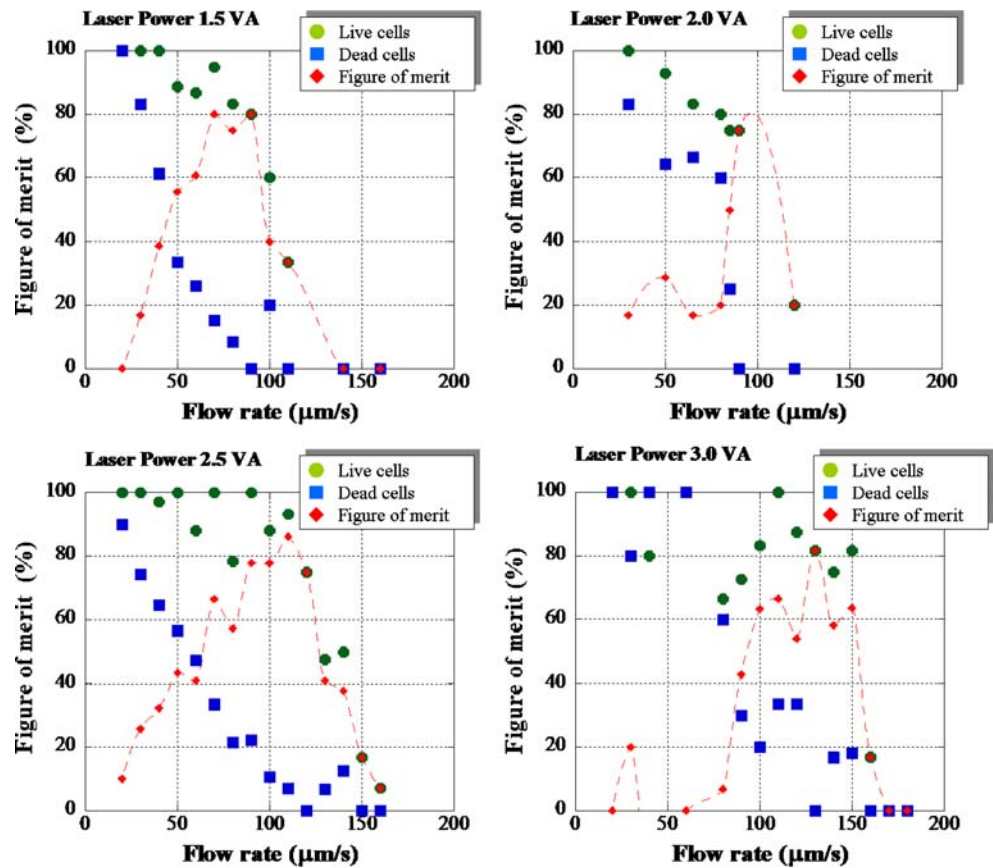


Fig. 4 Picture frames showing separation of dead and live cells by using optical trapping in a microchannel. **a** Live and dead cells flow from *left to right*. **b,d** A live cell is trapped by the laser light and its trajectory is changed. **c** A dead cell is not trapped and its original trajectory is maintained

Difference in refractive index of the particle and surrounding medium causes weak momentum change of the photon [24]; this can also change the optical trapping force. To investigate this possibility, we measured optical trapping forces of polystyrene and glass beads of very similar size (diameter ca. 6 μm). The polystyrene beads have higher optical trapping force (5.1 pN) than the glass beads (4.0 pN). Considering the similarity in the beads' size and shape, the differences in optical trapping force can be attributed to the differences in their refractive index: 1.58 for the polystyrene beads and 1.51 for the glass beads. These results strongly support our previous claim that refractive index of the cells affected their optical trapping force. All our results from this series of investigations indicate that optical trapping force of cells is affected by their size, morphology, light absorption, and refractive index.

Optical trapping of sample cells in the sheath flow of a microchannel provides a chance for high-throughput cell separation. To achieve this, the target cells should have a trajectory different from that of the other cells in the sample. This means that by using optical trapping only target cells should be trapped and their trajectory changed, while the other nontarget cells are unaffected and maintain their original trajectory. For that, we must consider and estimate an optimum balance between flow rate (drag force)

Table 3 Optical trapping laser power-dependent cell separation efficiency

| Laser power (W) | Flow rate/ 10^{-2} ($\mu\text{L}/\text{min}$) | Figure of merit (%) | Purity (%) ^a | Recovery (%) ^b |
|-----------------|---|---------------------|-------------------------|---------------------------|
| 1.5 | 1.07 | 80.0 | 100 | 80.0 |
| 2.0 | 1.37 | 75.0 | 100 | 75.0 |
| 2.5 | 1.68 | 86.2 | 93.3 | 93.3 |
| 3.0 | 1.99 | 81.8 | 100 | 81.8 |

^a Purity = number of live cells altering their trajectory/total number of live and dead cells altering their trajectory

^b Recovery = number of live cells altering their trajectory/total number of live cells tested

of the cells and laser power (trapping force). Figure 3 shows that at each laser power there is an optimum flow rate for the separation of trypan blue-stained dead and unstained live HeLa cells, which is depicted as figure of merit (FOM), i.e., the trapping efficiency difference between unstained live and trypan blue-stained dead HeLa cells. At flow rates lower than the optimum (i.e., the flow rate affording the highest FOM) at each laser power, both unstained live and trypan blue-stained dead HeLa cells were captured by the laser beam and their trajectories were changed, resulting in poor cell separation. On the other hand, flow rates higher than the optimum prevented the cells from being trapped by the laser beam and good separation was not attained. At the optimum flow rate, highly precise cell separation between unstained live and trypan blue-stained dead HeLa cells was attained, as shown in Table 3. Unstained live HeLa cells were captured by the optical trap and their trajectories changed, while trypan blue-stained dead HeLa cells were not captured and maintained their original trajectory, as shown in Fig. 4. Thus, it is important to consider the optimum flow rate at each laser power to achieve good cell separation. In addition, Table 3 indicates that within the experimental conditions increasing laser power makes it possible to separate the cells in a shorter time without much loss of separation efficiency. Of course, increasing laser power above certain levels may damage the cells, even though in this study we could not find any critical damage to the cells; therefore, it is highly desirable to select appropriate laser powers after considering whether activity of the separated cells is important.

Our method introduced here has a cell separation accuracy of 75% or higher, which is comparable to that typically achieved by conventional FACS (>80%). However, the sample handling capacity (ca. 1 cell/s) of our approach is much lower than that of conventional FACS (ca. 7×10^4 cells/s) because of the intrinsic limitation of the microfluidic approach. Microfluidic systems are designed to handle very small volumes of sample and are unsuitable for handling large amounts of sample. In fact, FACS combined with a microchip system has a sample handling

capacity of ca. 10 cells/s [8], which is not superior than that of our method considering the expansivity of our method. Further optimization of microchip design and experimental conditions may lead much higher sample handling capacity as well as higher separation accuracy.

Conclusions

We investigated properties of cells affecting their optical trapping and successfully established a novel cell separation method based on the combined use of optical trapping and microchips. A sheath flow of sample solutions created in the microchip made the sample cells flow in a narrow linear stream and an optical trap created by a highly focused laser beam captured only the target cells and altered their trajectory. Through a series of investigations, we clarified that the morphology, size, light absorption, and refractive index of cells affect their optical trapping force. In addition, we demonstrated that there is an optimum balance between optical trapping force and sample flow rate for high separation efficiency. Our results clearly indicate that we can achieve high-efficiency cell separation if one or more of the abovementioned properties (morphology, size, light absorption, and refractive index) are largely different, without special sample pretreatments such as cell staining, concentration, and purification, which is hardly achievable by other separation methods. In addition, optical trapping in microchips requires small amounts of sample and minimized sample treatments, and permits high-throughput cell separation and integration of other functions on the chips. We are now developing microchips integrated with other functions for optical trapping-based higher-performance cell separation. We will report further integrated cell separation methods with optical trapping and microchips for biological samples in a forthcoming article.

Acknowledgements The present work was supported in part through Special Coordination Funds for Promoting Science and Technology of the Ministry of Education, Culture, Sports, Science and Technology, the Japanese Government.

References

1. Nagrath S, Sequist LV, Maheswaran S, Bell DW, Irimia D, Ulkus L, Smith MR, Kwak EL, Digumarthy S, Muzikansky A, Ryan P, Balis L, Tompkins RG, Haber DA, Toner M (2007) *Nature* 450:1235–1239
2. Friedman SL, Roll FJ (1987) *Anal Biochem* 161:207–218
3. Tulp A, Verwoerd D, Pieters J (1993) *Electrophoresis* 14:1295–1301
4. Miltenyi S, Muller W, Weichel W, Radbruch A (1990) *Cytometry* 11:231–238
5. Malatesta P, Hartfuss E, Götz M (2000) *Development* 127:5253–5263
6. El-Ali J, Sorger PK, Jensen KF (2006) *Nature* 442:403–411
7. Furdul VI, Harrison DJ (2004) *Lab Chip* 4:614–618
8. Fu AY, Spence C, Scherer A, Arnold FH, Quake SR (1999) *Nature* 17:1109–1111
9. Becker FF, Wang XB, Huang YPR, Pethig R, Vykoukal J, Gascoyne PRC (1995) *Proc Natl Acad Sci USA* 92:860–864
10. Yamada M, Kasim V, Nakashima M, Edahiro J, Seki M (2004) *Biotechnol Bioeng* 88:489–494
11. Chang WC, Lee LP, Liepmann D (2005) *Lab Chip* 5:64–73
12. Huang LR, Cox EC, Austin RH, Sturm JC (2004) *Science* 304:987–990
13. Ashkin A (1970) *Phys Rev Lett* 24:156–159
14. Ashkin A, Dziedzic JM (1971) *Appl Phys Lett* 19:283–285
15. Ashkin A, Dziedzic JM (1987) *Science* 235:1517–1520
16. Ashkin A, Dziedzic JM, Yamane T (1987) *Nature* 330:769–771
17. Hirano K, Baba Y, Matsuzawa Y, Mizuno A (2002) *Appl Phys Lett* 80:515–517
18. Hirano K, Nagata H, Ishido T, Tanaka Y, Baba Y, Ishikawa M (2008) *Anal Chem* 80:5197–5202
19. Nagata H, Tabuchi M, Hirano K, Baba Y (2005) *Electrophoresis* 26:2247–2253
20. D’Helon C, Dearden EW, Rubinsztein-Dunlop H, Heckenberg NR (1994) *J Mod Opt* 41:595–601
21. Schönle A, Hell SW (1998) *Opt Lett* 23:325–327
22. Liu Y, Cheng DK, Sonek GJ, Berns MW, Chapman CF, Tromberg BJ (1995) *Biophys J* 68:2137–2144
23. Peterman EJG, Gittes F, Schmidt CF (2003) *Biophys J* 84:1308–1316
24. Sato S, Inaba H (1994) *Opt Lett* 19:927–929
25. Liu Y, Sonek GJ, Berns MW, König K, Tromberg BJ (1995) *Opt Lett* 20:2246–2248